

## Oligoacene exciton binding energies: Their dependence on molecular size

Kerstin Hummer and Claudia Ambrosch-Draxl\*

*Institut für Physik, Universität Graz, Universitätsplatz 5, 8010 Graz, Austria*

(Received 4 November 2004; published 17 February 2005)

We show how the optical absorption properties of organic molecular crystals based on finite molecular units depend on the oligomer length. We calculate the dielectric tensor for the first four linear oligoacenes by solving the Bethe-Salpeter equation for the electron-hole Green's function. The exciton binding energy significantly decreases with the molecular size. While strongly bound excitons are present in naphthalene, the carriers are only weakly bound in pentacene. This trend is understood in terms of the increasing dielectric screening and the spatial distribution of the exciton wave function.

DOI: 10.1103/PhysRevB.71.081202

PACS number(s): 78.40.Me, 71.35.Cc

A variety of measurements have been performed on the linear oligoacenes to determine their electronic and optical properties, e.g., carrier mobilities<sup>1,2</sup> and photoconductivity,<sup>3</sup> in view of their applicability in organic thin-film transistors and optoelectronic devices.<sup>4,5</sup> However, the question on the exciton binding energies in such organic semiconductors is still controversial and hence, of great interest. Regarding this problem, the organic polymers have been comprehensively studied in the past, but a consensus could not be achieved up to now. In general, there exist different opinions, whether the lowest optical transition is due to the absorption of free charge carriers (direct interband transitions), weakly bound electron-hole (*e-h*) pairs (Wannier or charge transfer excitons), or tightly bound (Frenkel) excitons. In this context, the exciton binding energy (BE) varies from a few  $k_B T$  to the order of 1 eV even within one material (e.g., poly-*para*-phenylene-vinylene).<sup>6,7</sup> On the way to solving this puzzle, a first success has been achieved by *ab initio* calculations: It has been found that the interchain interaction can reduce the exciton BE up to one order of magnitude and that the excitons extend over several unit cells along the chain.<sup>8-10</sup> In organic crystals built of shorter molecular units it is still believed that the intermolecular interactions are weak and therefore the *e-h* pairs are expected to be basically confined to single molecules resulting in large exciton BEs. In a previous work on anthracene<sup>11</sup> it has indeed been shown that the lowest excitation is generated by a strongly bound *e-h* pair. However, systematic quantitative first-principles studies on the size dependence of the exciton BE in such molecular crystals are still missing. At the same time, high crystallinity can hardly be achieved in polymers, such that in real samples chain fragments of different lengths are present. Therefore, the investigation of the excitonic effects as a function of the molecular size is extremely important. This motivated the calculations of exciton binding energies for the series of linear oligoacenes presented in this work.

We apply the full-potential augmented plane wave plus local orbitals (APW+lo) formalism<sup>12</sup> as implemented in the WIEN2K code<sup>13</sup> for the ground state and the EXCITING@WIEN2K package<sup>14</sup> for the description of the optical properties. Exchange and correlation effects have been treated by the generalized gradient approximation. The materials considered are naphthalene (2A), anthracene (3A), tet-

racene (4A), and pentacene (5A), where  $n$  in  $nA$  indicates the number of phenyl rings in the molecule and hence measures the oligomer length. At ambient conditions, 2A and 3A crystallize in the monoclinic structure  $P2_1/a$ , whereas 4A and 5A have the triclinic space group  $P1$ . All four materials exhibit a herringbone pattern of molecules in the unit cell. The lattice parameters of  $nA$ , which have served as input for the calculations, are taken from Refs. 15–18. In a preceding step, the internal geometry of these crystal phases has been optimized, i.e., the atomic positions have been relaxed by minimizing the forces acting on the atoms to be less than 2 mRy/a.u. Based on these structures, the imaginary parts of the dielectric tensors  $\text{Im } \epsilon_{ii}(\omega)$  have been calculated within the random-phase approximation (RPA).<sup>19</sup> Concerning the crystalline structure it is emphasized that the  $y(z)$  Cartesian components of the dielectric tensor are equivalent to the  $b$ - and the  $c$ -axis polarized transitions in 2A and 3A. In triclinic 4A and 5A, however, only the  $c$  axis remains parallel to the Cartesian  $z$  axis. For 5A it has been shown<sup>20</sup> that the transformation of the  $y$  into the  $b$  component does not significantly change the spectrum in the energy range of interest.

Since the RPA describes the excitation spectra of solids only in a single-particle picture, excitons are not present in such calculations. Therefore, the Bethe-Salpeter equation (BSE) for the two-particle Green's function<sup>21,22</sup> has been solved, which allows for the treatment of the *e-h* Coulomb interaction. An elaborate description of this formalism is given in Ref. 23. Regarding the following discussion of our results, the most important equations are briefly summarized here. The matrix eigenvalue form of the BSE is given by

$$\sum_{v'c'k'} \hat{H}_{vc\mathbf{k},v'c'\mathbf{k}'}^{\text{eff}} A_{v'c'\mathbf{k}'}^\lambda = E^\lambda A_{vc\mathbf{k}}^\lambda, \quad (1)$$

where the crucial step is to set up the effective Hamiltonian  $\hat{H}^{\text{eff}}$ . The indices  $v(c)$  and  $\mathbf{k}$  stand for the valence (conduction) band and a vector  $\mathbf{k}$  in the irreducible Brillouin zone. Its diagonalization yields the eigenvalues  $E^\lambda$  and eigenvectors  $A_{vc\mathbf{k}}^\lambda$  representing the excitation energy of the  $\lambda$ -th correlated *e-h* pair and the coupling coefficient used to construct the exciton wave function, respectively.  $\hat{H}^{\text{eff}}$  consists of three terms,

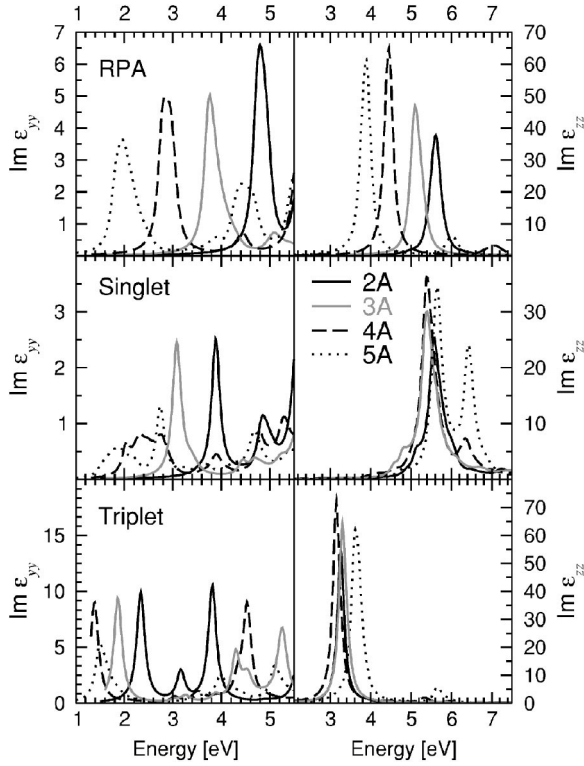


FIG. 1.  $y$  and  $z$  component of the  $\text{Im } \varepsilon_{ii}(\omega)$  calculated for  $nA$  within the RPA (upper panels) and the BSE formalism (lower panels). A lifetime broadening of 0.1 eV has been included.

$$\hat{H}_{vc\mathbf{k},v'c'\mathbf{k}'}^{\text{eff}} = \hat{H}_{vc\mathbf{k},v'c'\mathbf{k}'}^{\text{diag}} + \hat{H}_{vc\mathbf{k},v'c'\mathbf{k}'}^{\text{dir}} + 2\hat{H}_{vc\mathbf{k},v'c'\mathbf{k}'}^{\text{x}} \quad (2)$$

The kinetic term  $\hat{H}^{\text{diag}}$  is determined from the quasiparticle energies, while the attractive direct and the repulsive exchange interaction matrix elements,  $\hat{H}^{\text{dir}}$  and  $\hat{H}^{\text{x}}$ , are responsible for the formation of bound excitons. The  $\hat{H}^{\text{dir}}$  contains the statically screened Coulomb interaction, whereas in the  $\hat{H}^{\text{x}}$  the bare Coulomb potential without the long-range part is present. Note that the latter is not active for spin triplet excitations. In the calculation of the  $\text{Im } \varepsilon_{ii}(\omega)$ , the valence and conduction state energies have been approximated by the Kohn-Sham eigenvalues corrected by a  $\mathbf{k}$ -independent self-energy (scissors operator) such that for each material the calculated optical gap matches the experimentally observed one. Recent GW calculations on pentacene<sup>24</sup> have shown that the self-energy correction to the band gap is roughly  $\mathbf{k}$  independent in an energy window plus to minus 5 eV around the Fermi level justifying the applicability of the scissors approximation.

In the following we present the calculated optical absorption behavior for the series of oligoacenes and discuss the spin singlet and triplet binding energies as well as the singlet-triplet ( $S$ - $T$ ) splitting as a function of the oligomer length and the polarization of the exciting radiation. In Fig. 1 the two major Cartesian components of  $\text{Im } \varepsilon_{ii}(\omega)$ , i.e., the  $y$ - and the  $z$ -axis polarized response, are depicted. The important features of these spectra are summarized in Table I together with experimental findings.<sup>25,26</sup> Let us first focus on

TABLE I. Lowest  $y$ - and  $z$ -polarized response of the oligoacenes: The calculated peak positions and exciton BEs compared to experiment (Refs. 25 and 26, and references therein).

Peaks (eV)	2A	3A	4A	5A
Theory				
RPA <sub><math>y</math></sub>	4.8	3.8	2.8	2.0
$S_y$	3.9	3.1	2.4	1.9
$T_y$	2.4	1.9	1.4	1.5
RPA <sub><math>z</math></sub>	5.6	5.1	4.5	3.9
$S_z$	5.6	5.4	5.4	5.6
$T_z$	3.3	3.3	3.2	3.6
Experiment				
Band gap	5.0–5.4	3.9–4.2	2.9–3.4	2.2–2.4
$T_y$	2.6	1.9	1.3	0.8
$S_y$	3.9–4.0	3.1–3.5	2.4–3.0	1.9–2.3
$S_z$	5.6	5.7–6.0	5.4–5.6	5.4
Theory				
SBE <sub><math>y</math></sub>	1.0–1.5	0.4–1.1	0.1–1.0	0.0–0.5
TBE <sub><math>y</math></sub>	2.4–2.8	2.0–2.3	1.6–2.1	1.4–1.6
$S_y$ - $T_y$	1.3–1.4	1.2–1.6	1.1–1.7	1.1–1.5
$S_z$ - $S_y$	1.6–1.7	2.2–2.9	2.4–3.2	3.1–3.5

the RPA results. For the whole series, the lowest, but weak optical transition is generated by  $y$ -axis polarized light, whereas the strong absorption next in energy is due to  $z$ -axis polarized radiation. These optical transitions are shifted to lower energies, when the molecular size increases. Analogous to the oligophenylenes,<sup>27</sup> this redshift is in accordance with the reduction of the band gap within the series and depends almost linearly on the inverse of  $n$ .

If the  $e$ - $h$  Coulomb interaction is included in the theoretical description, the spin singlet ( $S$ ) and triplet ( $T$ ) exciton response is obtained. In the following we denote the energy difference between the  $S$  peak position and the RPA peak as the singlet exciton binding energy (SBE). The triplet exciton binding energy (TBE) is analogously specified. In 2A, an SBE <sub>$y$</sub>  of 0.9 eV is calculated. With increasing  $n$ , SBE <sub>$y$</sub>  decreases to 0.66, 0.44, and 0.09 eV in 3A, 4A, and 5A, respectively. Comparing our results for 5A to Ref. 24, we find a lower singlet as well as triplet binding energy. We note here that a small part of the difference can be attributed to the different definition of the BE. Since the BEs are sensitive to the underlying ground-state calculations and the molecular geometry, it is hard to explicitly trace back discrepancies.

The reduction of the SBE <sub>$y$</sub>  can be explained in terms of the following two effects: The longer the molecule is, the more the  $e$ - $h$  pair can spread out and thereby the average

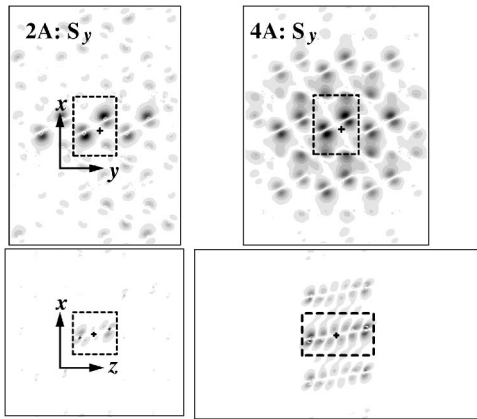


FIG. 2. The 2D electron distribution  $|\psi_{ck}(\mathbf{r}_e)|$  of  $S_y$  with respect to the hole at a fixed position (dark cross) calculated for 2A and 4A. The unit cell is indicated by dashed rectangles. These  $xy$  ( $xz$ ) maps represent slices at  $z=0.3$  ( $y=0.3$ ) with the hole located at  $z=0$  ( $y=0$ ) in units of  $c$  ( $b$ ). The dark regions correspond to high density.

Coulomb attraction is reduced. At the same time, the dielectric screening becomes more effective. For this reason, the exciton binding energy exhibits a decrease faster than  $1/n$  making free  $e-h$  pairs possible for larger molecules. In the following, we attribute the details of the optical spectra to the respective terms in the effective Hamiltonian. While the interplay of both, the screened attractive ( $\hat{H}^{\text{dir}}$ ) and the unscreened repulsive ( $\hat{H}^{\text{x}}$ ) Coulomb terms influences the SBE, the TBE is only governed by the former. Therefore, the TBE generally reduces more drastically than the SBE. E.g., TBE<sub>y</sub> decreases by 1.9 eV, when going from 2A to 5A. The effect of  $\hat{H}^{\text{x}}$  is reflected in the  $S_y$ - $T_y$  splitting, because the singlet and the triplet Hamiltonian are distinguished only by this term. We see that also  $\hat{H}^{\text{x}}$  is weakened, since the  $S_y$ - $T_y$  splitting reduces with increasing  $n$ , however only by half the amount of TBE<sub>y</sub>, i.e., by 0.9 eV between 2A and 5A.

The importance of the dielectric screening is also demonstrated by the exciton wave function. In Fig. 2 the 2D electron distribution  $|\psi_{ck}(\mathbf{r}_e)|$  of  $S_y$  is shown for 2A and 4A. In 2A the exciton is extended over more than one unit cells in the  $y$  direction, but rather localized in  $x$  and  $z$  thus giving rise to the sizeable singlet exciton BE. When going from 2A to 4A, the exciton is still confined to one molecule along  $z$ , which, however, increases considerably in size, but significantly expands along  $x$ . This means that the  $e-h$  pair preferably extends in the herringbone ( $xy$ ) plane instead of the molecular plane.

Compared to the  $y$ -polarized spectra, pronounced differences are observed in the  $z$  component of the dielectric tensors, when the  $S_z$  and  $T_z$  energies are analyzed. First of all, it is significant that in the whole series strongly bound spin singlet excitons are not present in this channel. For example, the energy of  $S_z$  in 2A is identical to that of the corresponding RPA peak resulting in a zero BE. Therefrom it can be concluded, that the attractive term  $\hat{H}^{\text{dir}}$  is compensated by the repulsive  $\hat{H}^{\text{x}}$ . Further looking at the details of the  $z$ -polarized response reveals that both these interactions decrease with increasing  $n$ , but not to the same amount as found for the

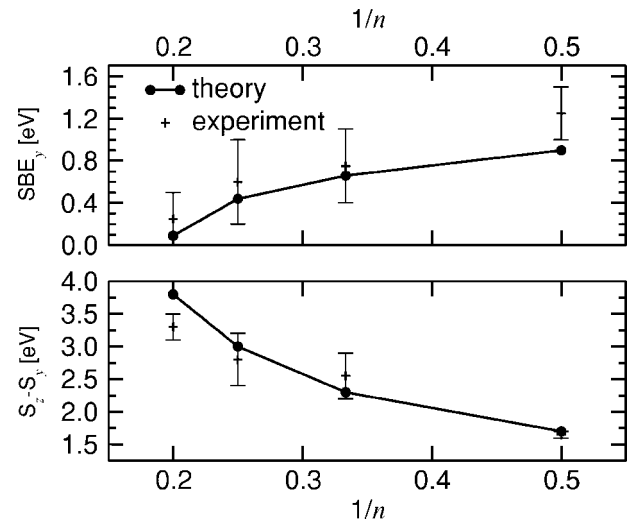


FIG. 3. The  $SBE_y$  and the  $S_z$ - $S_y$  splitting as a function of  $1/n$  in comparison to experiment.

$y$ -polarized  $e-h$  pairs. This time the reduction of the attractive part is roughly six times larger than that of the repulsive exchange interaction. As a consequence, the latter even overcompensates the former, which explains the much smaller redshifts of the  $S_z$  and  $T_z$  spectra between 2A and 4A and finally the blueshift of these peaks in case of 5A. When comparing the  $S_y$ - $T_y$  splitting and the  $S_z$ - $T_z$  splitting, we find that the latter is significantly larger in magnitude, but less changing with the molecular size, which can also be attributed to this effect.

Let us now discuss the calculated results in comparison to the experimental findings, which are summarized in Table I and Fig. 3. The calculated quantities,  $SBE_y$  and the relative position of  $S_y$  with respect to  $S_z$ , which we call the  $S_z$ - $S_y$  splitting, are in good agreement with the data extracted from measurements. Unlike  $SBE_y$ , the  $S_z$ - $S_y$  splitting increases as a function of  $n$ . It is more than twice as large in 5A compared to 2A, since contrary to  $S_y$ ,  $S_z$  hardly changes. Moreover, the reduction of the exciton BE with increasing  $n$  is supported by available measurements. When comparing theory and experiment, however, we have to consider the following facts, which may be responsible for certain discrepancies: Regarding theory, the calculations are performed for perfect crystals based on experimental structural data. Further, the electron-phonon interaction, which has been proposed to be important in such materials,<sup>28</sup> cannot be treated on the same footing and thus is not included in our studies. The solution of the BSE gives rise to an accuracy of 0.1 eV for the exciton BEs. Concerning experiment, we want to emphasize that not only single crystals, but also crystalline thin films are used, which are extremely difficult to grow with a high degree of crystallinity and purity for the shorter linear oligoacenes. Moreover, polymorphism in the samples could explain the large error bars in the experimental values. E.g., in pentacene also a crystalline  $V$  phase has been refined<sup>29</sup> that preferably exists in vapor deposited thin films. We want to emphasize that our calculation of pentacene is based on the single-crystal structure<sup>18</sup> denoted as  $S$  phase. The fact, that the  $SBE_y$  of 5A is higher in several (but not all) of the experiments does not

necessarily mean a discrepancy. From Ref. 24 it is known that the energy gaps of the  $S$  and  $V$  phase differ by 0.3 eV. Indeed, the experimental band gap given in Table I refers to the  $S$  phase, such that the energy gap is deduced to be 1.9 eV for the  $V$  phase. Assuming that in Table I the 1.9 eV for  $S_y$  corresponds to  $V$  and the value of 2.3 eV to the  $S$  structure, the resulting measured  $SBE_y$  of 5A would be approximately zero. Such uncertainties also affect the positions of  $S_z$  and  $T_y$ , hence providing a possible explanation for the deviation of the  $S_z$ - $S_y$  splitting in 5A.

Summarizing our findings, we have addressed the questions of how the oligomer length influences the optical absorption properties of organic molecular crystals based on finite molecules by studying linear oligoacenes. In the monoclinic structures the lowest optical transition is generated by a strongly bound spin singlet exciton. But with increasing molecular size, the exciton binding energy is very effectively reduced. Therefore, the spin singlet exciton is rather weakly bound in pentacene. This is a consequence of the decreasing  $e$ - $h$  Coulomb interaction with longer molecules, which can

be attributed to two effects: the expansion of the  $e$ - $h$  wave function and the strong enhancement of the dielectric screening. For this reason, the reduction of the  $e$ - $h$  binding energy is faster than the decrease of the band gap in these materials and thus making free charge carriers possible for  $n$  greater than six. As a consequence, the chain fragments of real polymer samples should not particularly differ from the infinite chains in their optical behavior. Besides, if the light is polarized parallel to the  $z$  axis, bound  $e$ - $h$  pairs are not present in the investigated series, but the strong optical transitions are due to free carriers. Thus not only the molecular size, but also the polarization of the exciting radiation considerably influence the size of the exciton BE. Such a behavior has been found only in the oligoacenes so far and may be an important issue for their potential in technological applications.

This work was supported by the Austrian Science Fund (Project No. 16227-PHY) and by the EU RT network *EXCITING*, Contract No. HPRN-CT-2002-00317.

\*Email address: claudia.ambrosch@uni-graz.at

<sup>1</sup>N. Karl, *Synth. Met.* **133-134**, 649 (2003).

<sup>2</sup>N. Karl and J. Marktanner, *Mol. Cryst. Liq. Cryst. Sci. Technol., Sect. A* **355**, 149 (2001).

<sup>3</sup>Z. Rang, A. Haraldsson, D. M. Kim, P. P. Ruden, M. I. Nathan, R. J. Chesterfield, and C. D. Frisbie, *Appl. Phys. Lett.* **79**, 2731 (2001).

<sup>4</sup>C. D. Dimitrakopoulos and D. J. Mascaro, *IBM J. Res. Dev.* **45**, 11 (2001).

<sup>5</sup>L. Torsi, N. Cioffi, C. D. Franco, L. Sabatini, P. G. Zambonin, and T. Bleve-Zacheo, *Solid-State Electron.* **45**, 1479 (2001).

<sup>6</sup>D. Moses, J. Wang, A. J. Heeger, N. Kirova, and S. Brazovskii, *Synth. Met.* **125**, 93 (2002).

<sup>7</sup>S. V. Frolov, Z. Bao, M. Wohlgenannt, and Z. V. Vardeny, *Phys. Rev. Lett.* **85**, 2196 (2000).

<sup>8</sup>J.-W. van der Horst, P. A. Bobbert, M. A. J. Michels, G. Brocks, and P. J. Kelly, *Phys. Rev. Lett.* **83**, 4413 (1999).

<sup>9</sup>A. Ruini, M. J. Caldas, G. Bussi, and E. Molinari, *Phys. Rev. Lett.* **88**, 206403 (2002).

<sup>10</sup>P. Puschnig and C. Ambrosch-Draxl, *Phys. Rev. Lett.* **89**, 056405 (2002).

<sup>11</sup>K. Hummer, P. Puschnig, and C. Ambrosch-Draxl, *Phys. Rev. Lett.* **92**, 147402 (2004).

<sup>12</sup>E. Sjöstedt, L. Nordström, and D. J. Singh, *Solid State Commun.* **114**, 15 (2000).

<sup>13</sup>P. Blaha, K. Schwarz, G. K. H. Madsen, D. Kvasnicka, and J. Luitz, WIEN2K (Vienna University of Technology, Vienna, 2001).

<sup>14</sup>Code development under the EU RT network *EXCITING*, <http://www.exciting.physics.at>

<sup>15</sup>D. W. J. Cruickshank, *Acta Crystallogr.* **10**, 504 (1957).

<sup>16</sup>R. Mason, *Acta Crystallogr.* **17**, 547 (1964).

<sup>17</sup>J. M. Robertson, V. C. Sinclair, and J. Trotter, *Acta Crystallogr.* **14**, 697 (1961).

<sup>18</sup>R. B. Campbell, J. M. Robertson, and J. Trotter, *Acta Crystallogr.* **14**, 705 (1961).

<sup>19</sup>H. Ehrenreich and M. H. Cohen, *Phys. Rev.* **115**, 786 (1959).

<sup>20</sup>K. Hummer, *On the Electro-optical Properties of Oligo-acenes* (Shaker-Verlag Aachen, 2004).

<sup>21</sup>L. Sham and T. Rice, *Phys. Rev.* **144**, 708 (1966).

<sup>22</sup>M. Rohlfling and S. G. Louie, *Phys. Rev. Lett.* **81**, 2312 (1998).

<sup>23</sup>P. Puschnig and C. Ambrosch-Draxl, *Phys. Rev. B* **66**, 165105 (2002).

<sup>24</sup>M. L. Tiago, J. E. Northrup, and S. G. Louie, *Phys. Rev. B* **67**, 115212 (2003).

<sup>25</sup>E. A. Silinsh, *Organic Molecular Crystals* (Springer-Verlag, Berlin, 1980).

<sup>26</sup>M. Pope and C. E. Swenberg, *Electronic Processes in Organic Crystals and Polymers* (Oxford University Press, New York, 1999).

<sup>27</sup>P. Puschnig and C. Ambrosch-Draxl, *Phys. Rev. B* **60**, 7891 (1999).

<sup>28</sup>V. Coropceanu, M. Malagoli, D. A. da Silva Filho, N. E. Gruhn, T. G. Bill, and J. L. Brédas, *Phys. Rev. Lett.* **89**, 275503 (2002).

<sup>29</sup>C. C. Matheus, A. B. Dros, J. Baas, G. T. Oostergetel, A. Meetsma, J. L. de Boer, and T. M. Palstra, *Synth. Met.* **138**, 475 (2003).